Available online at www.sciencedirect.com

ScienceDirect

Polymer 48 (2007) 6354–6365

polymer

www.elsevier.com/locate/polymer

Multiple morphologies of self-assembled star aggregates of amphiphilic PEO-*b*-PNPMA diblock copolymers in solution, synthesis and micellization

Xuezhi Tang, Yongchen Hu, Caiyuan Pan*

Department of Polymer Science and Engineering, University of Science and Technology of China, Hefei, Anhui 230026, PR China

Received 29 April 2007; received in revised form 22 July 2007; accepted 15 August 2007
Available online 19 August 2007

Abstract

Novel amphiphilic block copolymers, poly(ethylene oxide)-*b*-poly(*p*-nitrophenyl methacrylate) (PEO-*b*-PNPMA) with controlled molecular weights and narrow molecular weight distribution were successively synthesized by ATRP of NPMA using PEO–Br as initiator. Self-assembling of the diblock copolymer PEO_{113}-*b*-$PNPMA_{28}$ in the different solvent mixtures yielded various morphologies of star micelle-like aggregates, such as spheres, vesicles, cauliflower-like aggregates and rod-like aggregates, which are determined by the nature of the common solvents and the selective solvents. Thus the critical selective solvent contents and the solvent contents in PNPMA-rich phase were measured, and they have the following order: ethanol > methanol > water, and THF > CH_3NO_2 > DMSO. The probable self-assembling mechanism is discussed. This method is convenient for preparation of multiple morphological star micelle-like aggregates in solution, especially from the amphiphilic block copolymers with relatively longer block shell.

Keywords: Amphiphilic block copolymer micelles; Multiple morphologies; Self-assembly

1. Introduction

Generally, the micellar materials can be achieved by self-assembling of block copolymers in a selective solvent [1–3]. The formation of micelles is determined by the repulsion of soluble blocks and the conjugation between insoluble chains, and their stability in the solution is due to the interaction of the soluble chains with the solvent. Based on the relative sizes of core and shell in micelles, the micelles can be divided into two types: (1) "star" micelles with small cores consisting of short insoluble blocks and expanded coronas consisting of longer soluble blocks and (2) crew-cut micelles with larger cores and short coronal hairs, and they are formed from asymmetric block copolymers with relatively long insoluble block [3]. For examples, the star micelles and the crew-cut micelles were obtained from self-assembling of the poly(isoprene)$_{350}$-*b*-poly(2-cinnamoylethyl methacrylate)$_{178}$ and the poly(styrene)$_{500}$-*b*-poly(acrylic acid)$_{60}$, where the subscripts represent the number of repeating units in the block copolymers, in selective solvents [4,5].

The crew-cut micelles have been attracting much attention for their multiple morphologies in solution from spheres, to rods, to cylinders, to worm-like micelles, to vesicles, and to lamellae, and the systematic investigations on the formation of various morphologies were reported [6–19]. On the other hand, spherical star micelles were frequently observed, but their multiple morphologies have been rarely studied [20,21]. Study on the formation of various morphologies from block copolymers with longer soluble block and short insoluble block should be useful to control the diversiform architectures, and to find their potential applications. Generally, morphologies formed from self-assembling of copolymers are affected by many factors, such as copolymer composition [15,18,22–25] and initial concentration of the polymers [6,16,18,24–27], type and concentration of the additive ions (salt, acid or base) [7], concentration of the additive precipitant [14,26], the nature and composition of common and selective solvent used [17–26,28] and the characters of copolymers [29,30]. The morphology is controlled by a force balance

---

* Corresponding author.
E-mail address: pcy@ustc.edu.cn (C. Pan).

0032-3861/$ - see front matter © 2007 Elsevier Ltd. All rights reserved.
doi:10.1016/j.polymer.2007.08.030

involving mainly the stretching of the insoluble blocks in the core, the surface tension between the core and outside solvent and the repulsion among the corona chains during the micellization [31]. Thus the solvent and block copolymers are important factors influencing the force balance during the formation of the aggregates. Many copolymer–solvent systems for formation of various morphologies have been studied [20,21,32–35]. For examples, poly(butadiene)-*b*-PEO was self-assembled in water to form worm-like micelles [32]. Self-assembling of polystyrene-*b*-poly(4-vinylpyridine) (PS-*b*-P4VP) in water yielded micelles [33]. Liu's group used hexane to associate PS-*b*-poly(2-cinnamoylethyl methacrylate) chains into micelles [34]. Shi's group used a binary solvent mixture of acetone and water or deionized water and ethanol or deionized water and *N*,*N*-dimethylformamide (DMF) to associate PS-*b*-poly(acrylic acid) chains into various morphological aggregates [20,21]. All block copolymers studied included hydrophobic block that becomes hydrophobic core of the micelles formed from self-assembling in a selective solvent, even after core cross-linking reaction [32,36].

The *p*-nitrophenyl methacrylate (NPMA) can easily be substituted by amino group and hydrolyzed in alkaline solutions, the corresponding derivatives have important applications in biological and medical fields [37–40]. Our group reported the synthesis of well-defined block copoly(styrene-*b*-NPMA) (PS-*b*-PNPMA) by atom transfer radical polymerization (ATRP) [41–43]. Polyethylene oxide (PEO) is an inert synthetic polymer *in vivo*, and the amphiphilic block copolymers containing PEO are potentially useful for encapsulation of hydrophobic materials in an aqueous solution. So, it should be interesting to synthesize well-defined diblock copolymers, PNPMA-*b*-PEO, and to investigate their self-assembling in selective solvents. After partial core cross-linking reaction by ethylene diamine and following hydrolysis, the hydrophobic core will become hydrophilic. In this paper, we report the synthesis of novel well-defined block copolymers, PEO-*b*-PNPMA by ATRP, and multiple morphologies of self-assembled star aggregates of the PEO_{113}-*b*-$PNPMA_{28}$ block copolymer in different solvents are investigated.

2. Experimental section

2.1. Materials

Poly(ethylene oxide) monomethyl ether (PEO–OH) (Fluka) ($M_n = 5000$, $M_w/M_n = 1.01$) was used as received. CuBr was synthesized from $CuSO_4$, NaBr and Na_2SO_3, purified by stirring it in glacial acetic acid, washing with methanol, and then drying in vacuum. Triethyl amine (TEA) was distilled over KOH after refluxing overnight. The α-bromobutyryl chloride was prepared from the reaction of 2-bromobutyryl acid with thionyl chloride. ^1H NMR (300 MHz, $CDCl_3$), δ (TMS, ppm): 4.28 (t, 1*H*, C*H*Br), 2.03 (m, 2*H*, C*H*$_2$), 1.08 (t, 3*H*, C*H*$_3$). The NPMA was synthesized according to the method described in Refs. [41,44]. ^1H NMR (300 MHz, $CDCl_3$), δ (TMS, ppm): 8.30 (d, 2*H*, aromatic protons *ortho* to the nitro group), 7.30 (d, 2*H*, aromatic protons *meta* to the nitro group), 6.09 and 5.58 (s, 2*H*, $CH_2{=}C$), 1.95 (s, 3*H*, C*H*$_3$).

All other reagents were of analytical grade, purchased from Shanghai Chemical Reagents Co., China, and used as received without further purification. The membrane for dialysis bag (molecular weight cutoff of 8000) was purchased from HuaMei Chemical Reagents Co., China.

2.2. Synthesis of macro-initiator PEO–Br

The macro-initiator, bromine-terminated poly(ethylene oxide) was synthesized as follows. Into a 250-ml round-bottom flask equipped with a magnetic stirrer, PEO–OH (10 g, 0.002 mol) and anhydrous toluene (100 ml) were added. After azeotropic distillation for removal of trace of water, TEA (0.22 g, 0.002 mol) was added. When the mixture was cooled to 0 °C, α-bromobutyryl chloride (4.08 g, 0.02 mol) was added dropwise in 45 min. Then the reaction mixture was stirred at room temperature for 24 h. The salt formed was removed by filtration. After most volatile compounds were removed, precipitation was carried out by addition of the residue into excess of diethyl ether. The dried crude polymer was dissolved in saturated $NaHCO_3$ aqueous solution, and successive extraction with dichloromethane was performed. The organic layers were combined and dried over $MgSO_4$ for 24 h. After removal of the solvent under vacuum, the purified macro-initiator was afforded.

^1H NMR (300 MHz, $CDCl_3$), δ (TMS, ppm): 4.39 (COOC*H*$_2$); 4.28 (C*H*BrCOO); 3.65 (C*H*$_2$C*H*$_2$O); 3.38 (C*H*$_3$O); 2.03 (CH_3C*H*$_2$); 1.08 (C*H*$_3$$CH_2$).

2.3. Preparation of diblock copolymer PEO-b-PNPMA

According to the feed ratio in Table 1, CuBr, 2,2′-bipyridine (bpy), macro-initiator PEO–Br and NPMA were added successively into a 5-ml glass tube with a magnetic bar. The mixture was degassed by three freeze–pump–thaw cycles, and the tube was then sealed under vacuum. The sealed tube was placed in an oil bath at 90 °C. After polymerization was carried out for the prescribed time, the tube was cooled in ice-water, and then opened. The reaction mixture was dissolved in THF, and then the polymer solution obtained was passed through a short neutral alumina column. The polymer was precipitated from an excess of diethyl ether three times, followed by drying in a vacuum oven at 40 °C for 24 h.

Table 1
Results and conditions of ATRP of NPMA[a]

Sample no.	NPMA/PEO–Br/CuBr/bpy (molar ratio)	Time (h)	Conv (%)[b]	M_n[c]	M_w/M_n[c]
0				7670	1.01
1	48/1/1/3	11	57	17780	1.20
2	96/1/1/3	11	45	21740	1.15
3	144/1/1/3	11	43	25930	1.33

[a] Bulk polymerization; temperature: 90 °C.
[b] Conversions were measured by gravimetric method.
[c] Measured by GPC.

2.4. Self-assembling of PEO-b-PNPMA in different solutions

The block copolymer was dissolved in a common solvent, tetrahydrofuran (THF) or dimethyl sulfoxide (DMSO) or nitromethane, to yield a polymer concentration of 1 mg/g. Then the solution in a dialysis bag was dialyzed against different solvents dissolving PEO, such as methanol, ethanol or water, for one day, and then the final morphology was formed.

2.5. Measurement of critical selective solvent content for the polymer solution in various common solvents

The block copolymer, PEO_{113}-*b*-$PNPMA_{28}$ (10 mg) was dissolved in 10 g of common solvent (THF or DMSO or nitromethane). Then the selective solvent (methanol or ethanol or water) was added gradually into W_1 g of the solution until the clean solution became slightly cloudy suddenly. The solution formed was weighted (W_2). The content of the selective solvent in the solution at the onset turbidity is defined as critical selective solvent content (csc), and the csc was calculated according to $\mathrm{csc} = (W_2 - W_1)/W_2$. The 1 mg/g copolymer solution was diluted with a common solvent to yield solutions with concentrations of 0.5, 0.1 and 0.01 mg/g. Their csc values were measured using the same method.

2.6. Solvent content measurement in the PNPMA-rich phase

Homopoly(NPMA) (homo-PNPMA) with narrow molecular weight distribution was synthesized by ATRP method according to our previous synthetic procedure [41]. Its degree of polymerization was 24, which was calculated based on its ^1H NMR data. Homo-PNPMA was dissolved separately in THF, DMSO and CH_3NO_2 yielding the solutions with a concentration of 1 mg/g. Into this solution, a precipitator (methanol or ethanol or water) was then added slowly up to the critical selective solvent content (csc), at which the phase separation occurred. After standing for *ca.* 2 days, the PNPMA-rich phase was deposited at the bottom of the container, and the two phases were easily separated. The masses of the PNPMA-rich phase (W_{PS}) and the PNPMA (W_P) obtained from complete removal of solvent were weighted. The solvent content (C_{sp}) was calculated according to $C_{SP} = (W_{PS} - W_P)/W_{PS}$.

2.7. Characterization

^1H NMR spectra were measured on a Bruker DMX-300 nuclear magnetic resonance (NMR) instrument with chloroform-*d* ($CDCl_3$) or dimethyl sulfoxide-d_6 (DMSO-d_6) as solvent and tetramethylsilane (TMS) as an internal standard. Measurements of molecular mass and molecular mass distribution of the polymers were performed at 30 °C on a Waters 150C gel permeation chromatography (GPC) instrument equipped with micro-Styragel columns (500, 10^3, and 10^4 Å) and a refractive-index detector. Polystyrenes with narrow molecular weight distribution were used as calibration standards. THF was used as an eluent at a flow rate of 1.0 ml/min. Transmission electron microscopy (TEM) was performed on a JEM100-SX transmission electron microscope operating at an acceleration voltage of 200 kV. For the observations of the size and distribution of the copolymer aggregates, samples were prepared by depositing polymer solutions (about 1 mg/g) onto copper grids, which had been coated with a thin film of Formvar and then coated with carbon. Solvents were allowed to evaporate from the grids at atmospheric pressure and room temperature. The size and size distribution of aggregates were also measured by dynamic light scattering (DLS) carried out on a Malvern Zetasizer Nanao ZS90 with an He–Ne laser (633 nm) and 90° collecting optics. All measurements were carried out at 25 °C, and data were analyzed by Malvern Dispersion Technology Software 4.20.

3. Results and discussion

3.1. Preparation of diblock copolymer PEO-b-PNPMA

The diblock copolymer, PEO-*b*-PNPMA was prepared according to Scheme 1. The first step was the synthesis of macro-initiator, PEO–Br, by the reaction of PEO–OH with α-bromobutyryl chloride. For complete transformation of terminal hydroxyl group to initiating sites, excess of α-bromobutyryl chloride was used in the reaction. The unreacted α-bromobutyryl chloride was easier to be removed during the precipitation of polymer solution from diethyl ether. The

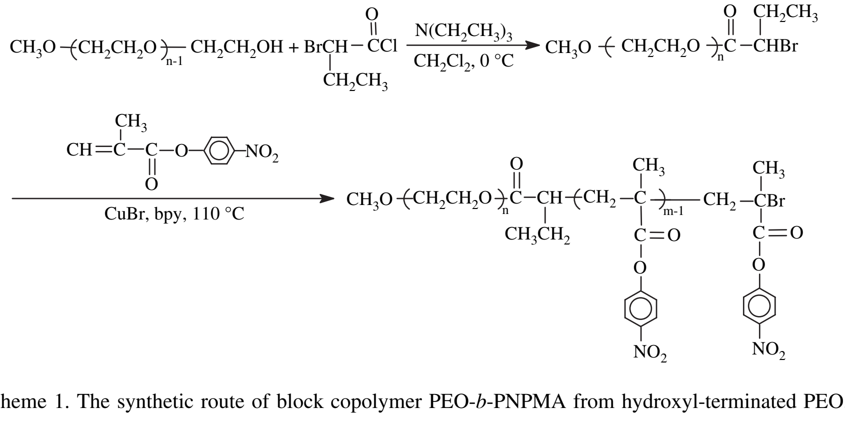

Scheme 1. The synthetic route of block copolymer PEO-*b*-PNPMA from hydroxyl-terminated PEO.

structure of macro-initiator was confirmed by its ^{1}H NMR spectrum. The number-average molecular mass, M_n(NMR), can be calculated based on the integration ratio of the signals at $\delta = 3.65$ ppm ($I_{3.65}$) to that at 4.39 ppm ($I_{4.39}$), and it was 5500, which is in accord with $M_n = 5000$ of PEO–OH. The GPC curve of the PEO–Br obtained is shown in Fig. 1A. The number-average molecular mass from GPC, $M_n(\text{GPC}) = 7670$, is much higher than $M_n(\text{NMR}) = 5500$. This might be attributed to different hydrodynamic volumes of PEO from that of polystyrene standards.

We reported in our previous papers [41–43] that NPMA could undergo block copolymerization of NPMA in bulk in the presence of macro-ATRP initiator, and the polymerization displayed "living" characters. Therefore, the diblock copolymers PEO-*b*-PNPMA were prepared by ATRP of NPMA using PEO–Br as macro-initiator and CuBr/bpy as catalyst and ligand, the conditions and results are listed in Table 1. The results in this table show that the molecular mass of block copolymer PEO-*b*-PNPMA could be controlled by the feed molar ratio of NPMA to PEO–Br in the same polymerization time, and the polydispersity is narrow. For bulk block copolymerization, the highest conversion was around 50% (57% conversion at lower feed molar ratio = 48/1 of NPMA to PEO–Br, 43% at higher feed ratio = 144/1), continuous polymerization after 11 h did not lead to obvious increase of conversion. Possible reason is too high viscosity of the higher molecular mass polymers formed. We could observe that the NPMA monomer was dissolved well in liquid PEO at 90 °C. With the evolution of polymerization, the PNPMA chains grew to higher molecular mass, viscosity of the system increased and successively the polymerization system became solid state. At this time the movements of propagating radicals, even NPMA monomer were restricted, and the propagation became difficult. In order to increase the conversion and to control the polymerization, we tried some solution polymerizations in various solvents. Unfortunately, the solvent, which is suitable for ATRP and can well-dissolve the polymers formed, was not found.

The GPC curves of the resultant polymers at various feeding ratios were measured, and a typical GPC curve (No. 2 in Table 1) is shown in Fig. 1B. In comparison with GPC curve of the PEO–Br shown in Fig. 1A, the unimodal GPC curve of the block copolymer (No. 2 in Table 1) appeared at high molecular mass position, demonstrating the occurrence of block copolymerization and the formation of block copolymers.

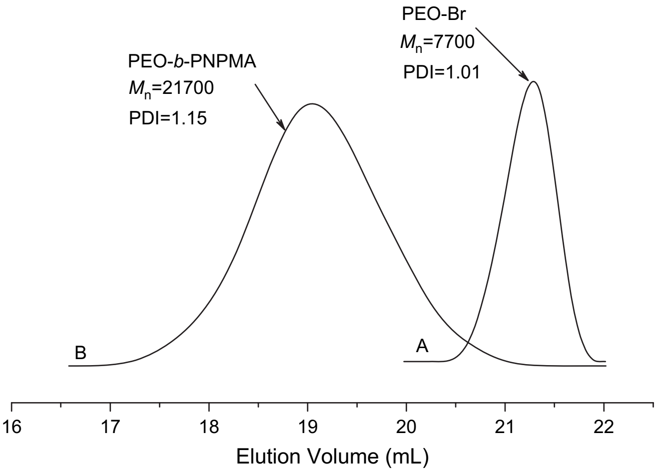

Fig. 1. Typical GPC traces of: (A) macro-initiator PEO–Br and (B) block copolymer PEO-*b*-PNPMA sample (No. 2 in Table 1).

To confirm the structure of the block copolymer obtained, the ^{1}H NMR spectra of copolymers were measured in DMSO-d_6, and a typical NMR curve of the sample (No. 2 in Table 1) is shown in Fig. 2. Except the characteristic signal of PEO at $\delta = 3.65$ ppm (d), we could find the characteristic signals of PNPMA block at $\delta = 1.02$–1.85 (e), 8.01–8.38 (a) and 7.07–7.53 ppm (b) corresponding to the protons of methyl, aromatic protons *ortho* and *meta* to the nitro group. The signal at $\delta = 2.02$–2.73 ppm (c) belonging to the methylene of PNPMA backbone was also observed. All these facts demonstrated that the block copolymer, PEO-*b*-PNPMA was obtained.

3.2. Micellization of copolymer

To study the effect of solvents on the morphology for the self-assembling of block copolymers, the sample PEO$_{113}$-*b*-PNPMA$_{28}$ (No. 2 in Table 1) with 113 EO and 28 NPMA units calculated on the basis of NMR spectra was used in this study. Its self-assembling was carried out in a binary solvent, mixture of common and selective solvents. The DMSO, THF and CH_3NO_2 were used as common solvents dissolving PEO and PNPMA; methanol, ethanol and water were used as selective solvents that dissolve PEO block only.

3.3. Critical selective solvent content and solvent content in the PNPMA-rich phase

Generally, two methods are used in the preparation of various assemblies from block copolymers [45]. The first is to dissolve the block copolymers in common solvent that is good for both blocks, successively gradual addition of

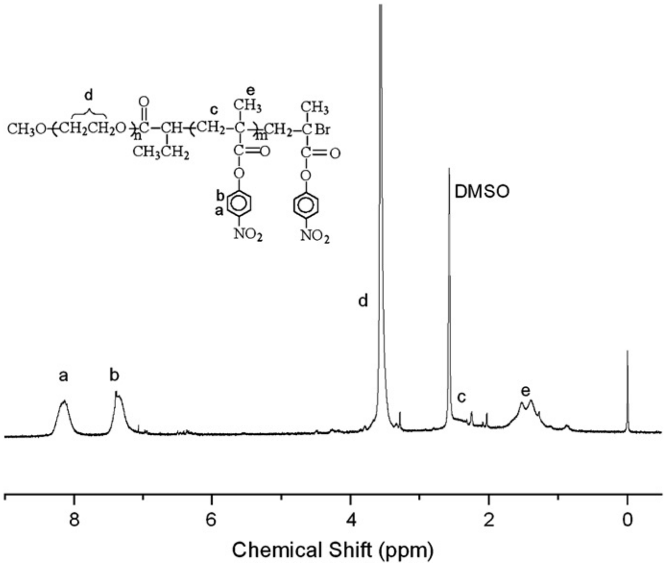

Fig. 2. ^{1}H NMR spectrum of PEO-*b*-PNPMA (No. 2 in Table 1) measured in DMSO-d_6.

a selective solvent into the copolymer solution. Eventually, the common solvent is stripped through the dialysis technique. The second is to dissolve the copolymers directly in a selective solvent. In either case, the nature and relative contents of the common solvents and the selective solvents are important factors influencing the morphologies formed. When a selective solvent is added into the polymer solution slowly, the microphase separation occurs. The relative selective solvent content at the onset turbidity of a polymer solution is defined as its critical selective solvent content (csc). Before we discussed the effect of solvents on the morphologies, a series of csc values were measured. In this study, DMSO, THF and CH_3NO_2 were used as common solvents for both blocks of the PEO-*b*-PNPMA copolymers, and methanol, ethanol and water were applied as selective solvents for the PEO block. Various csc values of the selective solvents for the PEO-*b*-PNPMA solution in DMSO, THF and CH_3NO_2 are shown in Fig. 3. We can see that the csc depends on the polymer

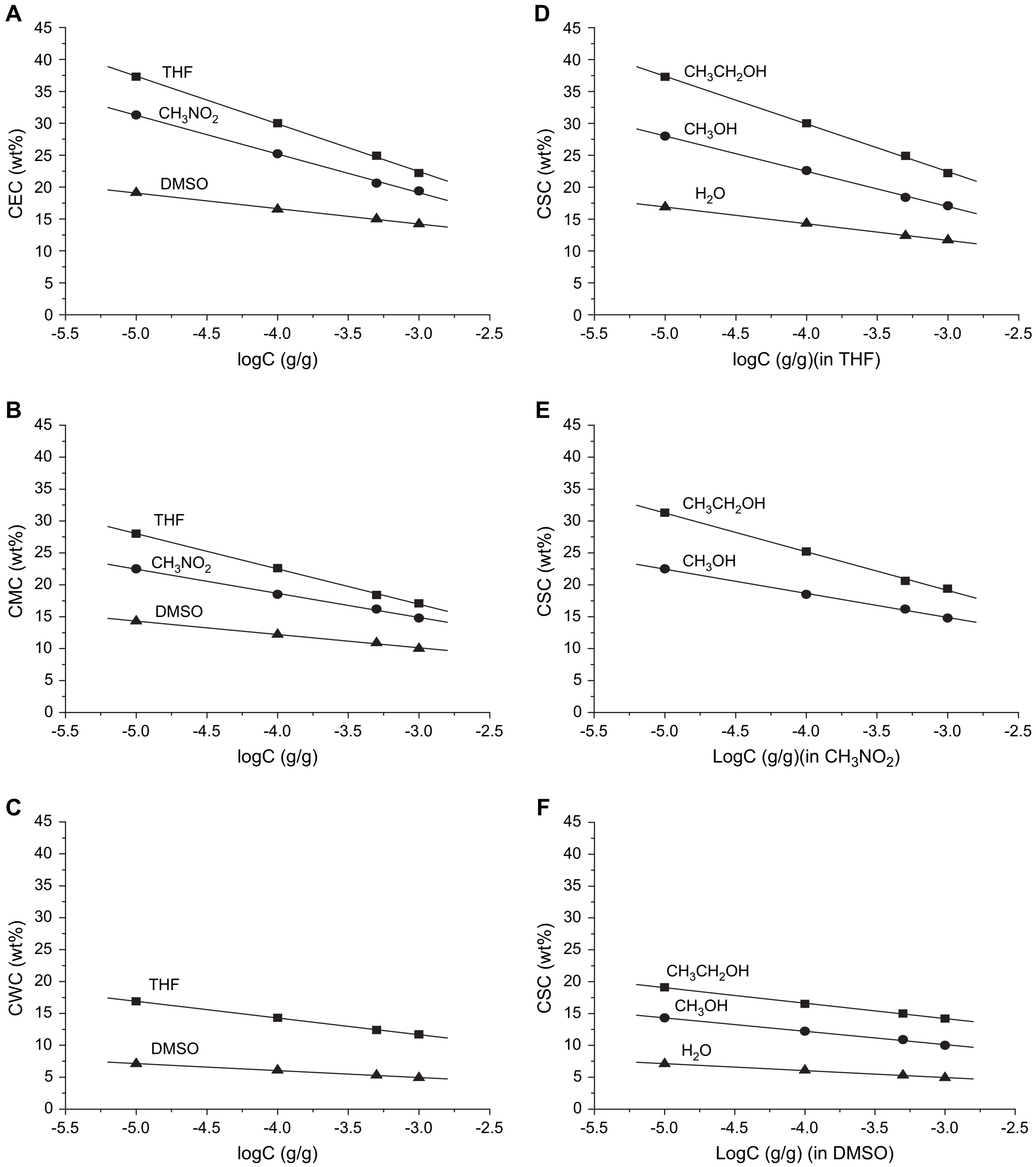

Fig. 3. Critical selective solvent contents *vs* logarithm of the polymer concentration for a solution of the copolymer PEO_{113}-*b*-$PNPMA_{28}$ in THF, CH_3NO_2 and DMSO using the same selective solvent, ethanol (A), methanol (B) and water (C) (E, M and W in CEC, CMC and CWC represent ethanol, methanol and water, respectively); and for the same copolymer solution in THF (D), CH_3NO_2 (E) and DMSO (F) using various selective solvents, ethanol, methanol and water (Fig. 3C and E has two lines due to the incompatibility between CH_3NO_2 and water).

concentration, and the higher the copolymer concentration is, the lower the csc. In addition, csc values are related to the nature of the common and selective solvents. For the same selective solvent, the csc values decreased from THF, to CH_3NO_2, to DMSO. For the same common solvent, the order of csc is ethanol > methanol > water.

Eisenberg's group pointed out that the aggregate morphologies of the amphiphlic block copolymer PS-*b*-PAA with longer PS block were changed with the variation of solvent content in the PS core [28]. In this study, the diblock copolymer that we used is PEO_{113}-*b*-$PNPMA_{28}$, in which the soluble PEO chains in the coronae are much longer than the insoluble PNPMA chains in the cores. The solvent content in the cores might affect morphologies of the aggregates. However, it is difficult in practice to quantify how much solvent the micelle cores contained. With the similar method used by Eisenberg's group [28,31], a $PNPMA_{24}$ similar to the chain length of PNPMA in the PEO_{113}-*b*-$PNPMA_{28}$ was used in the measurement. Although the solvent content in $PNPMA_{24}$-rich phase is probably somewhat different from that in the block copolymer, they should have the similar trend. The weight fractions of the solvents in various systems were measured, and the results are shown in Fig. 4. The results show the decrease of solvent content in the $PNPMA_{24}$-rich phase with the increase of the selective solvent content in the system. When the same selective solvent, ethanol or methanol or water was added into the same concentration of the $PNPMA_{24}$ solution in THF, CH_3NO_2 and DMSO, respectively, the solvent contents in $PNPMA_{24}$-rich phase decreased in the following order: THF > CH_3NO_2 > DMSO (Fig. 4A–C), that is, THF is the best solvent in the three common solvents. When the different selective solvents, ethanol, methanol and water were added respectively into the same concentration of $PNPMA_{24}$ in THF or CH_3NO_2 or DMSO, the solvent contents show the following order: ethanol > methanol > water (Fig. 4D and E). Thus water is the best precipitant of PNPMA in the three selective solvents.

3.4. Morphologies from self-assembling in mixture of DMSO and methanol or ethanol or water

To study the effect of solvent on the morphologies formed, the copolymer was dissolved in DMSO, and then the polymer solution was dialyzed against methanol or ethanol or deionized water, respectively, and the aggregates formed are shown in Fig. 5A, B and C. When the selective solvent is methanol, the resultant aggregates are dominantly core-shell spheres with diameter of about 20–25 nm. The average diameter measured by DLS is 24 nm (Fig. 6A). And a few vesicles with diameter of about 100 nm and the wall thickness of *ca.* 20 nm coexist as shown in Fig. 5A. When the selective solvent is ethanol, the resultant aggregates are vesicles with 118–138 nm in diameter and wall thickness of *ca.* 20 nm as shown in Fig. 5B. The vesicular morphology is evidenced from a higher transmission in the center of the aggregates than that of their periphery. The average diameter measured by DLS is 141 nm (Fig. 6B). However, when the copolymer solution was dialyzed against deionized water, core-shell cauliflower-like aggregates with diameter about 188–225 nm are formed as shown in Fig. 5C. They are consisted of loose micellar clusters, which is similar to that observed in Zhang's paper [20,21]. Fig. 6C shows that the average diameter of the aggregates measured by DLS is 213 nm. The results obtained from DLS measurements are in accord with that calculate from TEM images.

Various morphological micelle-like aggregates such as core-shell spheres, vesicles and core-shell cauliflower-like aggregates were formed when the copolymer solution in DMSO was dialyzed against methanol, ethanol and water. For understanding the effect of solvent on the formation of various morphologies, two factors might be considered: different dimensions or stretching degrees of the core-forming chains and different repulsive interactions between shell-forming chains in different common solvents during micellization [28]. Gradual replacement of the common solvent by selective solvents induced the variation of morphologies, this might result from change of PNPMA–solvent and PEO–solvent interaction. Generally, the strength of the polymer–solvent interaction is reflected by the χ parameter, which is related to the solubility parameter (δ) and the dielectric constant (ε). Table 2 listed the solubility parameters of the PEO and the solvents. The solubility of PNPMA is unknown, but the core-shell aggregates from the PEO_{113}-*b*-$PNPMA_{28}$ with much longer shell PEO chains and shorter PNPMA chains should have small cores and larger shell relatively. The effect of solvent on morphology is mainly determined by PEO–solvent interaction. The solubility parameter of ethanol ($\delta = 26.6\ \mathrm{MPa}^{1/2}$) is closer to that of PEO ($\delta = 19.9 \pm 2.2\ \mathrm{MPa}^{1/2}$) than that of methanol ($\delta = 29.7\ \mathrm{MPa}^{1/2}$). Therefore, the interaction between the PEO chains and ethanol should be stronger than that between the PEO chains and methanol. When DMSO in polymer solution was replaced by ethanol or methanol *via* dialysis, the solubility of mixture solvents, DMSO/ethanol decreased slower than that of DMSO/methanol (Fig. 4F). The aggregation of block copolymers in ethanol occurred at higher content of ethanol in the solvent mixture in comparison with methanol used as selective solvent (Fig. 3F). This led to the formation of larger vesicles with higher aggregation number and bigger dimension of the core in ethanol, and most of small core-shell spheres and small amount of larger vesicles were formed in methanol. The solubility parameter of water ($\delta = 47.9\ \mathrm{MPa}^{1/2}$) is much higher than that of PEO. But PEO could be dissolved in water probably due to intermolecular hydrogen bonds. When DMSO in the block copolymer solution was replaced by water, the solubility of PNPMA blocks in the mixture solvent decreased fast (Fig. 4F), aggregation of the polymer chains occurred at the lowest critical water content in the three selective solvents (Fig. 3F), forming small core-shell microspheres. With the increase of water, the solubility of mixture solvents DMSO/water decreased continually, the small microspheres could not exist stably, and their further aggregation yielded the core-shell cauliflower-like aggregates as shown in Fig. 5C.

In order to investigate the effect of PNPMA cross-linking on the aggregates, we cross-linked the vesicles formed from PEO_{113}-*b*-$PNPMA_{28}$ in DMSO/ethanol using ethylene

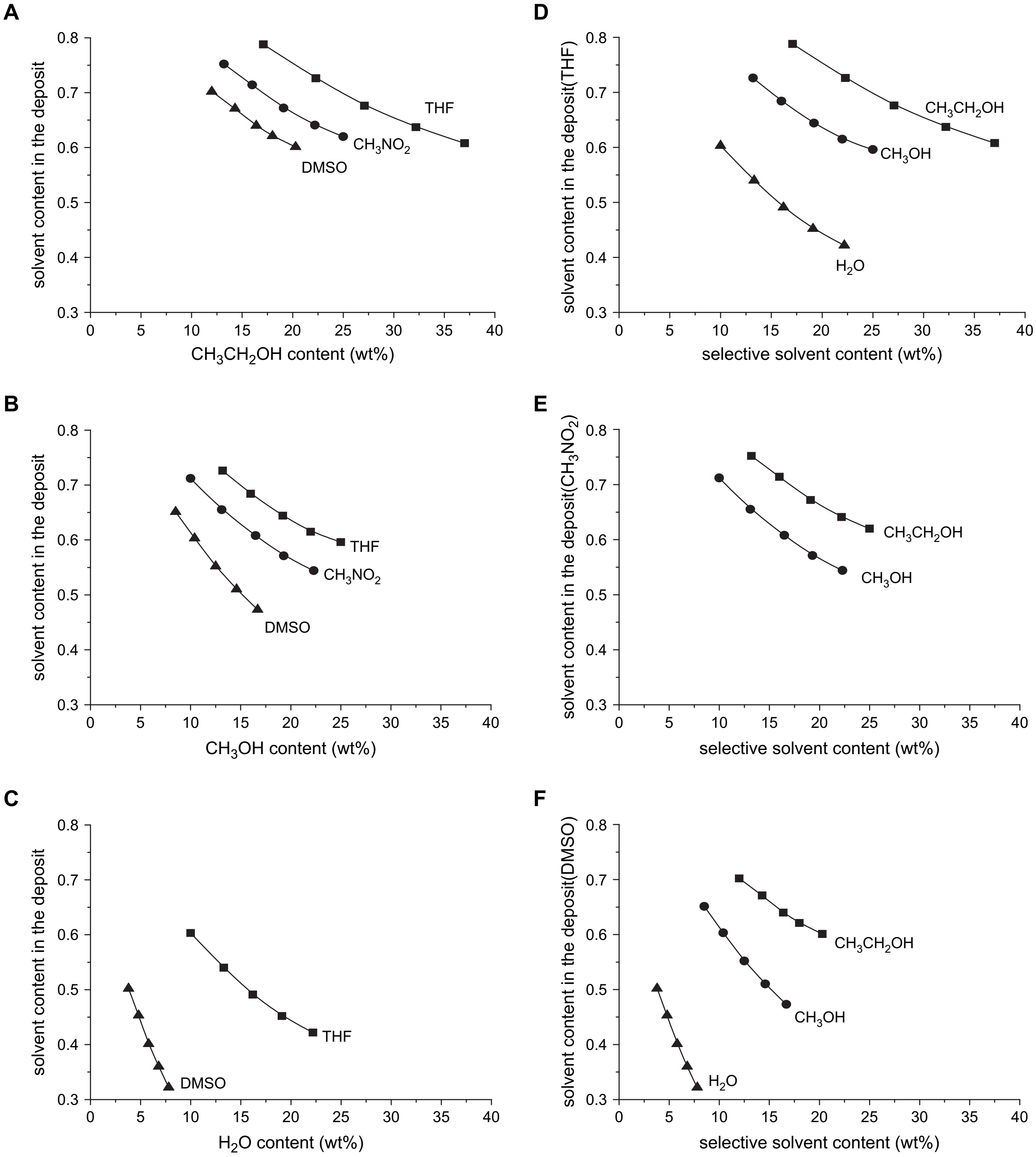

Fig. 4. Solvent content in the PNPMA-rich phase as a function of the selective solvent content in the solvent for the copolymer solutions in THF, CH_3NO_2 and DMSO using the same selective solvent, ethanol (A), methanol (B) and water (C); and for the same polymer solution in THF (D), CH_3NO_2 (E) and DMSO (F) using different selective solvents, ethanol, methanol and water (Fig. 4C and E has two curves due to the incompatibility between CH_3NO_2 and water).

diamine as cross-linking agent, and then the solution is dialyzed against ethanol. The TEM image of the aggregates after cross-linking is shown in Fig. 7A, and demonstrates that the vesicle morphology remained still. Their average diameter measured by DLS is 136 nm (Fig. 7B), which is slightly smaller than that of the aggregates before cross-linking (141 nm in Fig. 6B). This is reasonable because cross-linking will reduce the distance between PNPMA chains.

3.5. Morphologies from dialysis of PEO_{113}-b-$PNPMA_{28}$ solution in THF against methanol or ethanol or water

Among the three common solvents, THF is the best solvent for both blocks, PNPMA and PEO (Figs. 3A–C and 4A–C), and the PEO_{113}-*b*-$PNPMA_{28}$ can be dissolved in THF well. When the polymer solution was dialyzed against methanol, rod-like aggregates with diameter of *ca.* 20 nm and length of

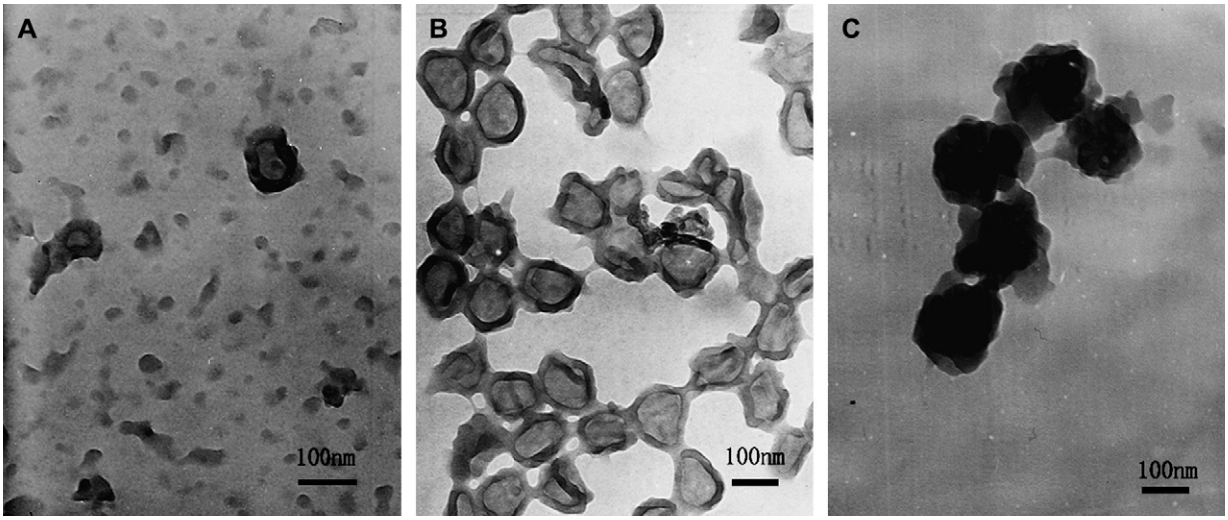

Fig. 5. TEM images of the PEO_{113}-*b*-$PNPMA_{28}$ aggregates made in DMSO with addition of different selective solvents, methanol (A), ethanol (B) and water (C) (the initial polymer solution was 0.1 wt%).

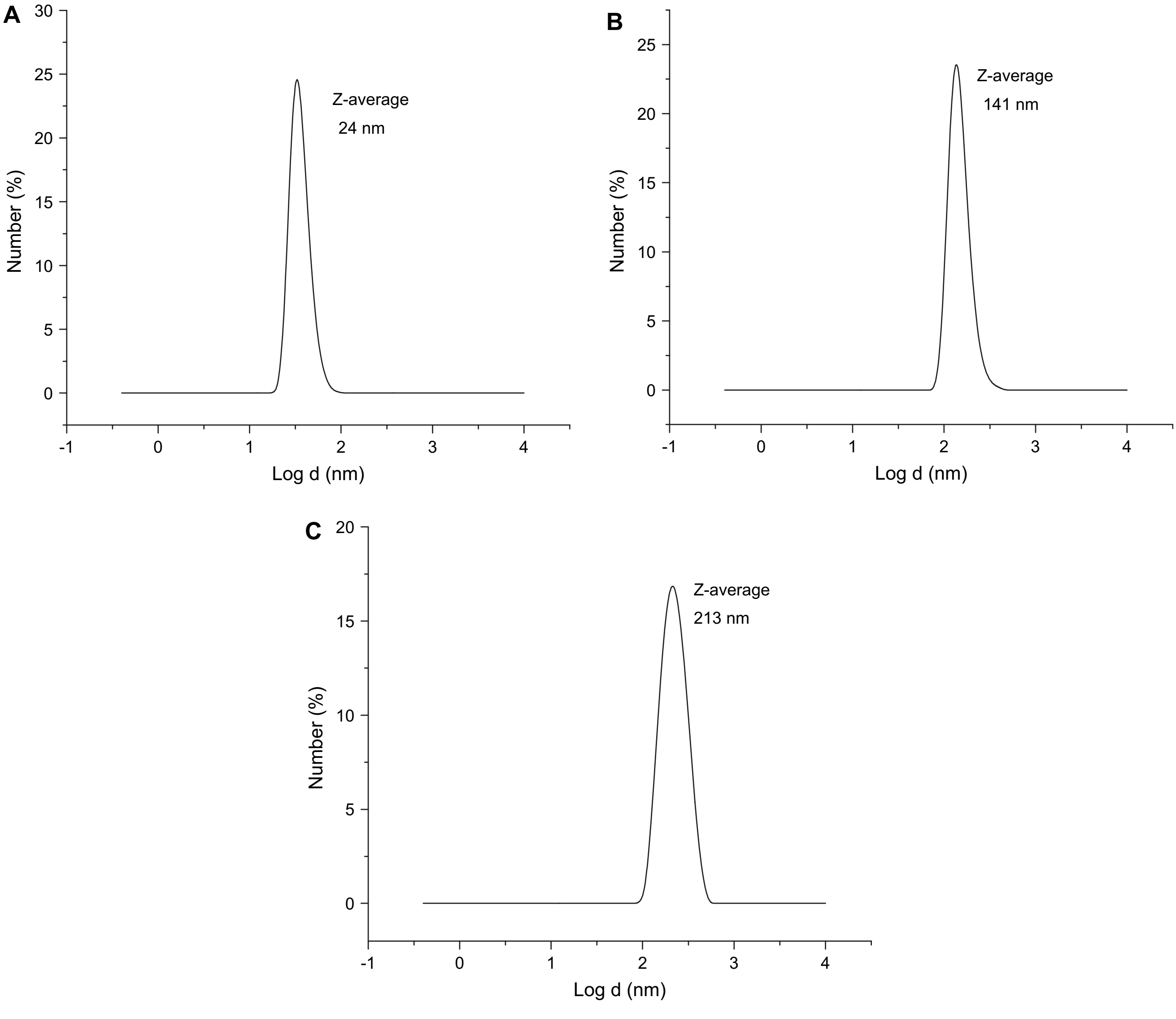

Fig. 6. Size distribution of the PEO_{113}-*b*-$PNPMA_{28}$ aggregates made in DMSO with addition of different selective solvents, (A) methanol, (B) ethanol and (C) water measured by DLS, $\theta = 90^\circ$.

Table 2
Solubility parameters of solvents and polymer [46]

Materials	Solubility parameters ($MPa^{1/2}$)			
	δ_d	δ_p	δ_h	δ
Poly(ethylene oxide)	17.3 ± 2	3.0 ± 1	9.4 ± 0.5	19.9 ± 2.2
DMSO	18.4	16.4	10.2	26.6
THF	16.8	5.7	8	19.4
CH_3NO_2	15.8	18.8	5.1	25
Methanol	15.1	12.3	22.3	29.7
Ethanol	15.8	8.8	19.4	26.6
Water	15.5	16.0	42.4	47.9

ca. 200 nm were observed as shown in Fig. 8A. Some rods have burls in the middle and branches. A few of small spheres with about 30 nm in diameter coexist in Fig. 8A. Dialysis of the polymer solution against ethanol formed worm-like micelles (interconnected rods) with diameter of about 20 nm as shown in Fig. 8B. In comparison with rod-like aggregates shown in Fig. 8A, the worm-like micelles are much longer, and no small sphere can be seen. When water was used as selective solvent, a bicontinuous structure of interconnected rods was obtained as shown in Fig. 8C. The average distance between two neighboring junctions is *ca.* 25 nm with approximately 15 nm in diameter. The whole structure has the largest size of about 400–500 nm in one direction. From its appearance and that of the shadowed regions, it can be judged that the structure is three dimensional and bicontinuous. A similar structure was observed from self-assembling of block copolymer, PSt_{190}-*b*-PAA_{20} in a water/DMF mixture [11].

As the selective solvent was changed from methanol to ethanol, and to water, various aggregate morphologies were observed from rods, to interconnect rods, to a bicontinuous structure of interconnected rods, respectively. The aggregates become more complicated and the degree of aggregation increases gradually with the variation of selective solvents. For explaining the transition of core-shell micelles to rods, two possible mechanisms as shown in Fig. 9 were proposed [14], the first involves a continuous insertion of single polymer chains into spherical micelles, leading to increases of the aggregation number and the core dimension. Finally, the micelles change the structure from spherical to rod-like. The second involves adhesive collisions of small spherical micelles, resulting in the increase of aggregation number and formation of larger spherical micelles. At last, the spherical micelles are transformed to rod-like. For both mechanisms, the first is the formation of spherical micelles, and then further chain insertion or adhesive micelle collisions leads to an increase in the length of rod-like aggregates, and then the morphology changes to rod-like. These mechanisms can be possibly used to explain the morphologies formed. A few of small spheres coexisting in Fig. 8A indicate the formation of micelles at first during the self-assembling. When DMSO and THF were used as common solvents, the solubility parameter of THF ($\delta = 19.4\ MPa^{1/2}$) is closer to that of PEO ($\delta = 19.9 \pm 2.2\ MPa^{1/2}$) than that of DMSO ($\delta = 26.6\ MPa^{1/2}$). THF is a better solvent for PEO chains than DMSO. When THF in polymer solution was replaced by selective solvents, the dimension of PEO corona in the mixture of THF/selective solvent is larger than that in the mixture of DMSO/selective solvent at the same conditions because of bigger repulsive interaction of the corona PEO chains in the former case. Thus core-shell micelles were formed for common solvent THF. With gradual replacement of THF in polymer solution by ethanol, the content of solvents in the cores of micelles decreased slowly (Fig. 4D) and higher CEC was obtained in comparison with CMC in the methanol case (Fig. 3D). The insertion of single polymer chains into core-shell aggregates was faster in the ethanol case due to higher mobility of the polymer chains in and out of the micelles. Therefore, longer rod-like aggregates were formed for dialysis of polymer solution in THF against ethanol. When water was used to replace THF in the polymer solution, aggregation of PNPMA chains formed small core-shell spherical micelles at lower CWC due to its bad solubility for PNPMA in comparison with other two selective solvents. The low chain mobility and weak interaction between PEO chains and solvent led to fast growth of the

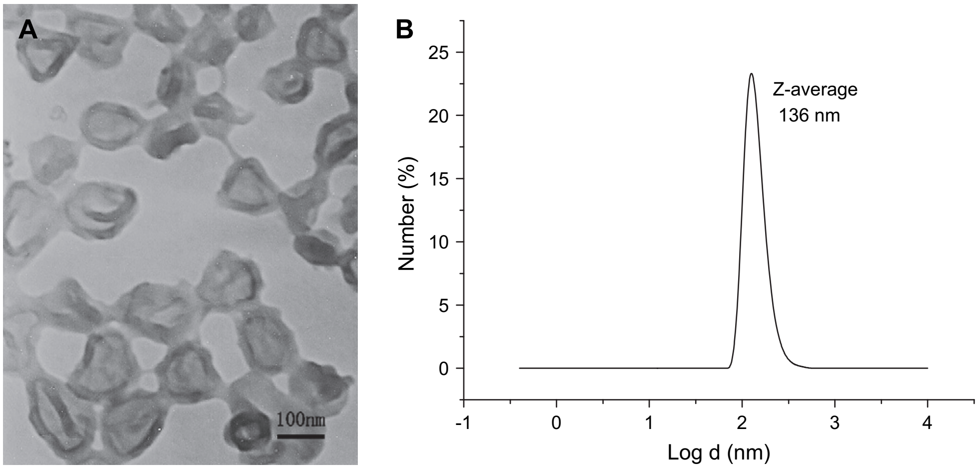

Fig. 7. TEM image (A) and size distribution (B) of the PEO_{113}-*b*-$PNPMA_{28}$ aggregates made in DMSO with addition of ethanol after cross-linking with ethylene diamine.

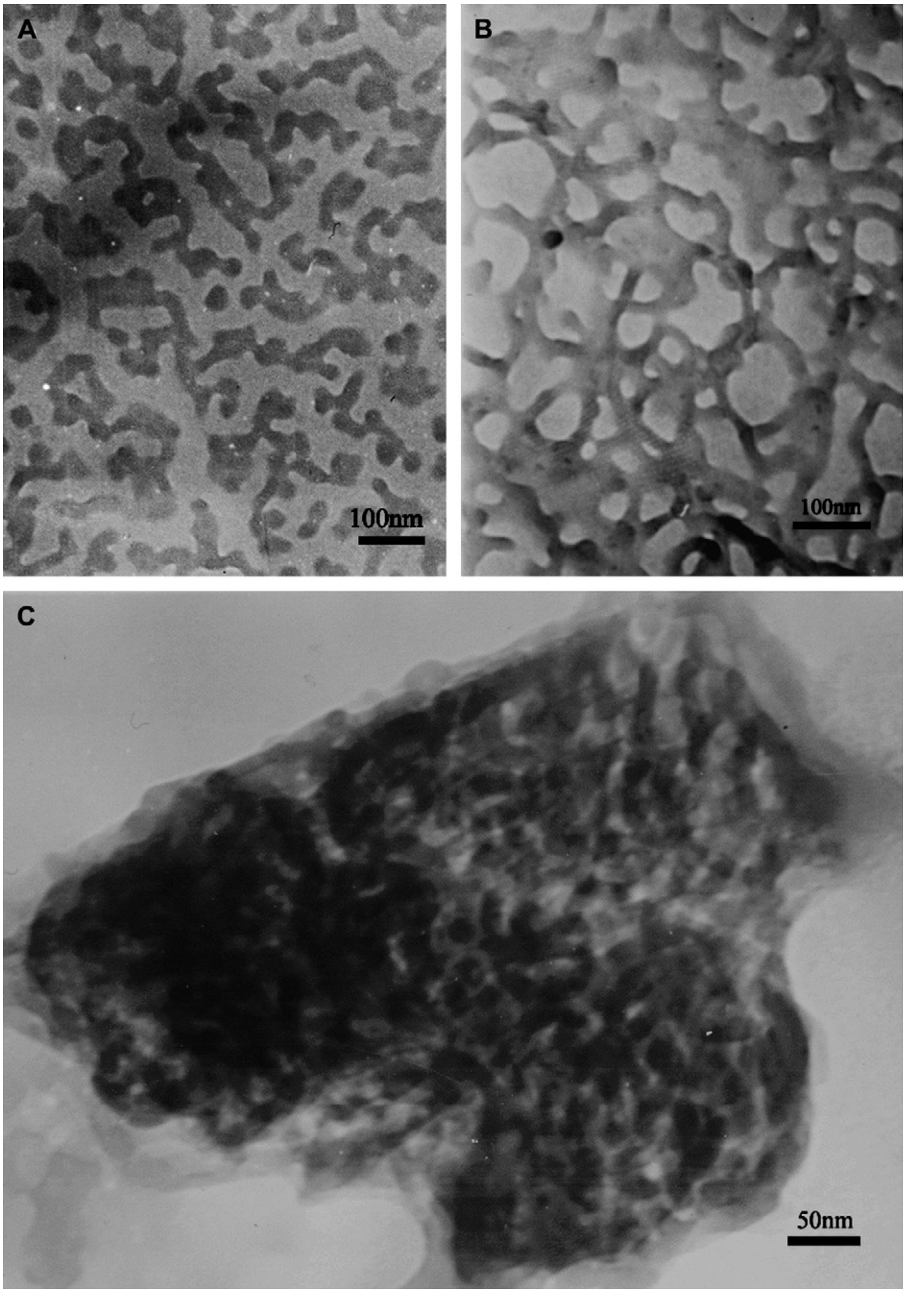

Fig. 8. TEM images of the PEO_{113}-*b*-$PNPMA_{28}$ aggregates made in THF with the addition of selective solvents, (A) methanol, (B) ethanol and (C) water (the initial polymer solution was 0.1 wt%).

rod-like aggregates, even though they interconnected with each other as shown in Fig. 8C.

3.6. Morphologies from dialysis of polymer solution in CH_3NO_2 against methanol or ethanol

When CH_3NO_2 was used as common solvent, only methanol and ethanol were selected as selective solvents because CH_3NO_2 and water are not compatible. The self-assemblies formed by dialysis of the PEO_{113}-*b*-$PNPMA_{28}$ solution in CH_3NO_2 against ethanol and methanol are shown in Fig. 10. In the methanol case, the aggregates in Fig. 10A are rods with burls and branches, their average diameter is about 15 nm, which are similar to that using THF and methanol as common and selective solvent (Fig. 8A). In the case of ethanol, bigger aggregates with a size of 100 nm were formed from the interconnected rods with diameter of 15 nm as shown in Fig. 10B, which is similar to the worm-like structure shown in Fig. 8B, but the size is smaller. The solubility parameter of CH_3NO_2 ($\delta = 25\ \mathrm{MPa}^{1/2}$) is lower than that of THF ($\delta = 19.4\ \mathrm{MPa}^{1/2}$), and higher than that of DMSO ($\delta = 26.6\ \mathrm{MPa}^{1/2}$). When CH_3NO_2 in polymer solution is gradually replaced by ethanol, its CEC and the solvent contents are lower than that of THF common solvent and higher than that of DMSO solvent (Figs. 3A and 4A). The solubility of CH_3NO_2/ethanol is between that of THF/ethanol and DMSO/ethanol, therefore

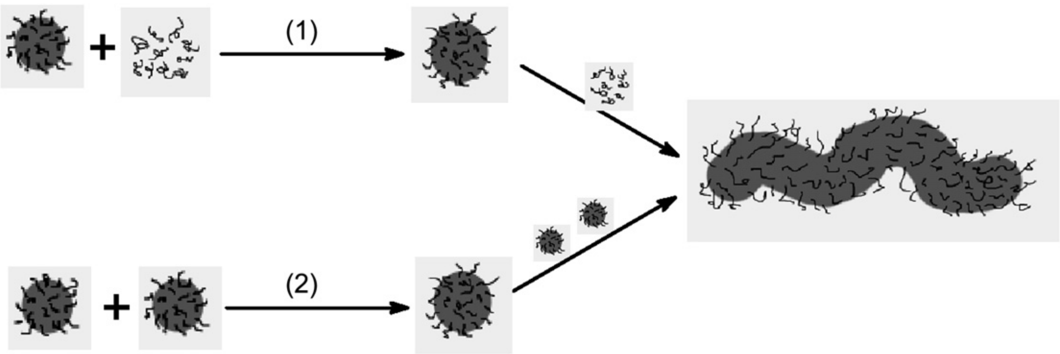

Fig. 9. Schematic drawing of two possible mechanisms for the formation of rod-like aggregates.

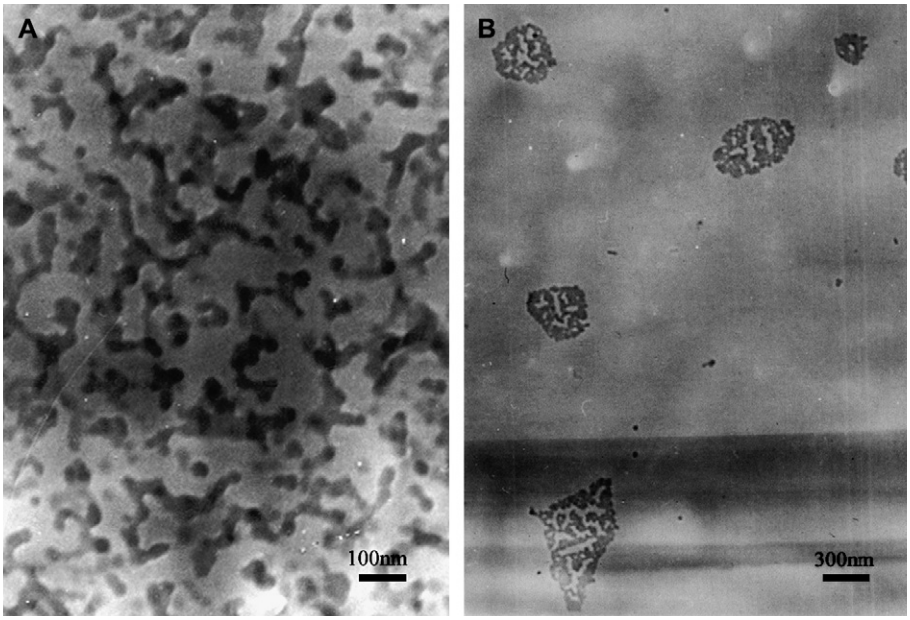

Fig. 10. TEM images of the PEO_{113}-*b*-$PNPMA_{28}$ aggregates made in CH_3NO_2 using different selective solvents, (A) methanol and (B) ethanol (the initial polymer solution was 0.1 wt%).

bigger aggregates composed of interconnected rods were formed, and they seem to be a transition aggregate between vesicles and worm-like aggregates.

4. Conclusions

A novel amphiphilic block copolymer consisting of poly(ethylene oxide) (PEO) and poly(*p*-nitrophenyl methacrylate) (PNPMA) was synthesized by ATRP of NPMA using PEO–Br as macro-initiator, and the molecular weights of the resultant PEO-*b*-PNPMA can be controlled from the molar ratio of monomer consumed to initiator, the molecular weight distribution is narrow. The interactions between polymer chains and solvents play important role in the formation of different morphologies. The PEO_{113}-*b*-$PNPMA_{28}$ morphologies formed in DMSO/ethanol, DMSO/methanol and DMSO/water change from vesicles to spherical micelles coexisted with small amount of vesicles, to cauliflower-like aggregates. This is related to the following solubility order of the solvents mixture: DMSO/ethanol > DMSO/methanol > DMSO/water. The critical selective solvent contents and the solvent contents in the PNPMA-rich phase have the same order. Dialysis of PEO_{113}-*b*-$PNPMA_{28}$ solution in THF against ethanol and methanol and water formed worm-like micelles (interconnected rods) and rod-like aggregates with burls and branches and bicontinuous structure of interconnected rods, respectively. Better compatibility of PEO-*b*-PNPMA with THF than that with DMSO leads to the transformation of micelles to rod-like aggregates. The strength difference of the polymer–solvent interaction induced different growth rates of rod-like aggregates, leading to the formation of those morphologies. The self-assembling in CH_3NO_2/ethanol and CH_3NO_2/methanol yielded the interconnected rods with small size and the rods with burls and branches, respectively.

This method is convenient for preparation of multiple morphological star micelle-like aggregates in solution, especially from amphiphilic block copolymers with relatively long shell block.

Acknowledgment

This work is supported by the National Natural Science Foundation of China under contract Nos. 50673086 and 50633010.

References

[1] Halperin A, Tirrell M, Lodge TP. Adv Polym Sci 1992;100:31.
[2] Webber SE. J Phys Chem B 1998;102:2618.
[3] Moffitt M, Khougaz K, Eisenberg A. Acc Chem Res 1996;29:95.
[4] Tao J, Liu G, Ding J, Yang M. Macromolecules 1997;30:4084.
[5] Zhao J, Allen C, Eisenberg A. Macromolecules 1997;30:7143.
[6] Zhang L, Eisenberg A. J Am Chem Soc 1996;118:3168.
[7] Zhang L, Eisenberg A. Macromolecules 1996;29:8805.
[8] Iyama K, Nose T. Polymer 1998;39:651.
[9] Tao J, Stewart S, Liu G, Yang M. Macromolecules 1997;30:2738.
[10] Yu K, Eisenberg A. Macromolecules 1996;29:6359.
[11] Yu K, Zhang L, Eisenberg A. Langmuir 1996;12:5980.
[12] Zhang L, Bartels C, Yu Y, Shen H, Eisenberg A. Phys Rev Lett 1997;79:5034.
[13] Luo L, Eisenberg A. J Am Chem Soc 2001;123:1012.
[14] Zhang L, Eisenberg A. Macromolecules 1999;32:2239.
[15] Li Z, Liang Y, Li F. Chem Commun 1999;16:1557.
[16] Liang Y, Li Z, Li F. Chem Lett 2000;4:320.
[17] Yuan J, Li Y, Li X, Cheng S, Jiang L, Feng L, et al. Eur Polym J 2003;39:767.
[18] Chen X, Ding X, Zheng Z, Peng Y. Macromol Biosci 2005;5:157.
[19] Riegel IC, Samios D, Petzhold CL, Eisenberg A. Polymer 2003;44:2117.
[20] Zhang W, Shi L, An Y, Gao L, Wu K, Ma R. Macromolecules 2004;37:2551.
[21] Zhang W, Shi L, An Y, Gao L, Wu K, Ma R, et al. Macromol Chem Phys 2004;205:2017.
[22] Ding J, Liu G, Yang M. Polymer 1997;38:5497.
[23] Maskos M. Polymer 2006;47:1172.
[24] Tung P-H, Kuo S-W, Chen S-C, Lin C-L, Chang F-C. Polymer 2007;48:3192.
[25] Jiang G, Wang L, Chen T, Yu H, Dong X, Chen C. Polymer 2005;46:9501.
[26] Zhou J, Wang L, Wang C, Chen T, Yu H, Yang Q. Polymer 2005;46:11157.
[27] Zhang L, Eisenberg A. Macromol Symp 1997;113:221.
[28] Yu Y, Zhang L, Eisenberg A. Macromolecules 1998;31:1144.
[29] Li T, Lin J, Chen T, Zhang S. Polymer 2006;47:4485.
[30] Liu X, Wu J, Kim J, Eisenberg A. Langmuir 2006;22:419.
[31] Zhang L, Eisenberg A. Polym Adv Technol 1998;9:677.
[32] Won YY, Davis HT, Bates FS. Science 1999;283:960.
[33] Shen H, Zhang L, Eisenberg A. J Am Chem Soc 1999;121:2728.
[34] Ding J, Liu G. Macromolecules 1997;30:655.
[35] Liang Y, Li Z, Li F. New J Chem 2000;24:323.
[36] Huang H, Kowalewski T, Remsen EE, Gertzmann R, Wooley KL. J Am Chem Soc 1997;119:11653.
[37] Bovin NV, Gabius H-J. Chem Soc Rev 1995;24:413.
[38] Zupan M, Karjnc P, Stavber S. J Polym Sci Part A Polym Chem 1998;36:1699.
[39] Ivanov AE, Zubov VP. J Chromatogr A 1994;673:159.
[40] Tadatomi N, Tutomu S, Toshiyuki H, Atushi S. J Polym Sci Part A Polym Chem 1989;27:2519.
[41] Liu Y, Wang L, Pan CY. Macromolecules 1999;32:8301.
[42] Liu Y, Wang L, Pan CY. Polymer 2002;43:7063.
[43] Pan CY, Tao L, Liu Y. Chin J Polym Sci 2002;20:353.
[44] Patai S, Bentov M, Reichmann ME. J Am Chem Soc 1952;74:845.
[45] Gérard R. Prog Polym Sci 2003;28:1107.
[46] Brandrup J, Immergut EH, Grulke EA. Polymer handbook. 4th ed., vol. 3. New York: Wiley-Interscience; 1999. p. VII 699–VII 701, VII 711.